ACS APPLIED MATERIALS & INTERFACES

Research Article

www.acsami.org

Chemical and Structural Investigation of High-Resolution Patterning with HafSOx

Richard P. Oleksak,[†] Rose E. Ruther,[†,‡] Feixiang Luo,[§] Kurtis C. Fairley,[∥] Shawn R. Decker,[‡] William F. Stickle,[⊥] Darren W. Johnson,[∥] Eric L. Garfunkel,[§] Gregory S. Herman,*,[†] and Douglas A. Keszler*,[‡]

[†]School of Chemical, Biological, and Environmental Engineering, Oregon State University, Corvallis, Oregon 97331-2072, United States

[‡]Department of Chemistry, Oregon State University, 153 Gilbert Hall, Corvallis, Oregon 97331-4003, United States

[§]Department of Chemistry and Chemical Biology, Rutgers, The State University of New Jersey, New Brunswick, New Jersey 08901-8554, United States

[∥]Department of Chemistry and Biochemistry, University of Oregon, Eugene, Oregon 97403-1253, United States

[⊥]Hewlett Packard Company, 1000 Northeast Circle Boulevard, Corvallis, Oregon 97330-4239, United States

ABSTRACT: High-resolution transmission electron microscopy (TEM) imaging and energy-dispersive X-ray spectroscopy (EDS) chemical mapping have been used to examine key processing steps that enable sub-20-nm lithographic patterning of the material $Hf(OH)_{4-2x-2y}(O_2)_x(SO_4)_y{\cdot}qH_2O$ (HafSOx). Results reveal that blanket films are smooth and chemically homogeneous. Upon exposure with an electron beam, the films become insoluble in aqueous tetramethylammonium hydroxide [TMAH(aq)]. The mobility of sulfate in the exposed films, however, remains high, because it is readily exchanged with hydroxide from the TMAH(aq) solution. Annealing the films after soaking in TMAH(aq) results in the formation of a dense hafnium hydroxide oxide material that can be converted to crystalline HfO_2 with a high electron-beam dose. A series of 9 nm lines is written with variable spacing to investigate the cross-sectional shape of the patterned lines and the residual material found between them.

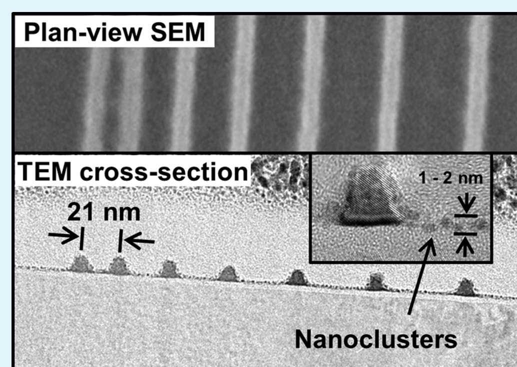

KEYWORDS: *inorganic resist, electron beam lithography, solution film deposition, hafnium oxide, thin film, cross-sectional TEM*

INTRODUCTION

In this contribution, we describe results from high-resolution imaging and chemical analysis of thin films and patterned structures of $Hf(OH)_{4-2x-2y}(O_2)_x(SO_4)_y{\cdot}qH_2O$, commonly known as HafSOx.[1] HafSOx is representative of a new approach involving the chemistry of nanosized inorganic clusters for addressing the resolution, line-width roughness (LWR), and sensitivity (RLS) trade-offs that limit lithographic performance of conventional organic materials at resolutions <20 nm.[2−4] Dense, sub-10-nm features have already been written with HafSOx using extreme ultraviolet (EUV) irradiation.[5] By examining films and structures derived from electron-beam exposures, we offer new insights into the HafSOx patterning process.

The small spot size and direct-write capabilities of electron-beam lithography make it a convenient method for studying nanopatterning at high resolution.[6] Organic materials, such as polymethyl methacrylate (PMMA),[7−9] ZEP-520,[10,11] and related chemically amplified resists,[12] are commonly employed to produce features at resolutions near 30 nm. In such systems, resolution is limited by the large radius of gyration of a polymer chain (2−4 nm) and photoacid diffusion in chemically amplified systems. These characteristics lead to high LWR (2−4 nm), which ultimately limits resolution. Smaller LWRs (<2 nm) have been demonstrated in inorganic materials, notably hydrogen silsequioxane (HSQ),[6,13] but this performance has come at the expense of poor sensitivities and long exposure times. The HafSOx system may offer a path for redefining the RLS triangle of conventional materials, because small LWRs and ultra-high-resolution features have been realized commensurate with relatively high sensitivities.[3] HafSOx uniquely affords these characteristics, because other Hf-based systems exhibit low resolution[14] and low sensitivity.[15]

The patterning capabilities and radiation sensitivity of HafSOx derive from the presence of Hf-bound peroxo ligands. The absorption of radiation leads to dissociation of the O−O bond of the peroxo group, which drives condensation reactions and a reduced solubility in exposed areas.[2] Unexposed areas of

Received: December 2, 2013
Accepted: February 6, 2014
Published: February 6, 2014

ACS Publications © 2014 American Chemical Society

a film may be readily dissolved in an appropriate developer, leaving a negative-tone pattern. The patterning process for HafSOx thus follows that of a conventional organic photoresist, involving some or all of the sequential steps: spin coat, post-application bake, exposure, post-exposure bake, development, and hard bake. Films and structures derived from selected steps in this flow have been characterized to develop an improved understanding of the overall process. As film thickness and feature size approach 10 nm and smaller, it becomes increasingly difficult to characterize in detail films and patterns using conventional methods, such as scanning electron microscopy.[16] In this study, we have used cross-sectional transmission electron microscopy (TEM) and energy-dispersive X-ray spectroscopy (EDS) to better assess these nano-dimensional features. In addition, the high atomic-number elements of the HafSOx system make these techniques especially useful for high-contrast imaging and chemical analysis. Because these characteristics are not commonly present in conventional patterning materials, e.g., organic resists, HafSOx presents a unique platform for studying lithographic patterning at near-atomic resolution.

■ EXPERIMENTAL SECTION

Stock solutions (1 M) were prepared by dissolution and dilution of $HfOCl_2·8H_2O$ (Alfa Aesar) and H_2SO_4(aq) (Mallinckrodt) with 18.2 MΩ purified water. Solutions for spin coating were prepared by adding 30 wt % H_2O_2(aq) (Macron) to the $HfOCl_2$(aq) solution, followed by sequential addition of H_2SO_4(aq) and 18.2 MΩ water. Final solutions were 0.15 M in hafnium, 0.105 M in sulfuric acid, and 0.45 M in hydrogen peroxide. Solutions were stable against precipitation for approximately 4 days at room temperature (depending upon the concentration) and several months when refrigerated. No change in film quality or reproducibility was observed for films deposited from aged, refrigerated solutions. Prior to spin coating, the substrates were treated with an O_2 plasma to improve wetting of the substrate. Films were deposited by dispensing solutions through a 0.45 μm filter and spin coating at 3000 rpm for 30 s. The films were then baked on a hot plate between 80 and 300 °C for 3−5 min. For patterning, films were baked at 80 °C for 3 min. Exposures were performed with a ZEISS Ultra-55 scanning electron microscope operating at 30 kV at a dose of 800 $\mu C/cm^2$. The microscope was equipped with a JC Nabity writing system for pattern generation. Unexposed and exposed films were soaked or developed at room temperature in 25 wt % tetramethylammonium hydroxide (TMAH, Alfa Aesar) for 30−60 s, thoroughly rinsed with 18.2 MΩ water, and baked at 300 °C for 3−5 min. A J. A. Woollam M-2000 spectroscopic ellipsometer was used to measure film thickness. Data were collected in 5° steps at incident angles covering the range of 55−65°. A Cauchy model was used to extract thickness. A FEI Titan G2 80-200 transmission electron microscope with ChemiSTEM operating at 200 kV was used for imaging and chemical analysis. TEM samples were prepared as cross-sections via focused-ion-beam lift-out using a FEI Quanta three-dimensional (3D) dual-beam scanning electron microscope. Approximately 30 nm of amorphous carbon were thermally evaporated on the sample to serve as a protective layer during the lift-out process. EDS line scans were taken in STEM mode, and the areas were correlated to bright-field TEM images that were acquired on nearby locations of the sample to avoid significant damage during STEM operation. The line scans were collected with a step size of 0.15−0.2 nm and then averaged over 1 nm to reduce noise. The scans were analyzed with Bruker Esprit 1.9 software using automatic background subtraction and quantification without standards. X-ray photoelectron spectroscopy (XPS) measurements were performed with a Thermo Scientific K-Alpha X-ray photoelectron spectrometer with an Al Kα (1486.7 eV) micro-focus monochromatic X-ray source and ultra-low energy electron flood gun. A 50 eV pass energy was used for high-resolution, element-specific XPS spectra. Spectra were analyzed with an Avantage XPS software package. All peaks were charge-corrected to adventitious hydrocarbon at 284.8 eV, and Au metal was used for energy scale calibration of the photoelectron spectrometer.

■ RESULTS AND DISCUSSION

Cross-sectional TEM images and associated STEM−EDS traces of a blanket-coated, unexposed HafSOx film (baked at 300 °C) are shown in Figure 1. From the bottom to the top,

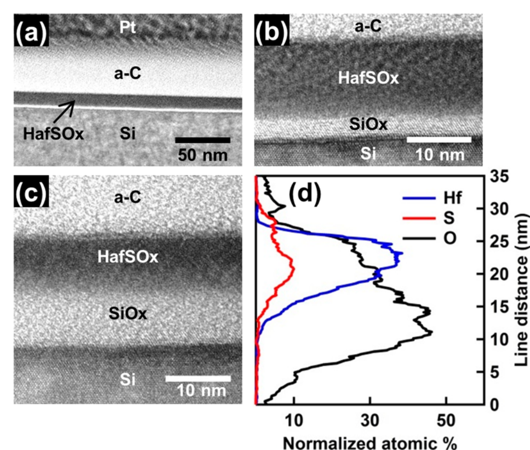

Figure 1. (a−c) Cross-sectional TEM images of the unexposed HafSOx film annealed at 300 °C and (d) STEM−EDS line scan aligned to panel c.

the material stack consists of the Si substrate, native silicon oxide, spin-coated HafSOx, and carbon/platinum protective layers. A low-magnification image (Figure 1a) reveals that the HafSOx film is smooth and very uniform. This uniformity is confirmed with a high-magnification image (Figure 1b), which was obtained immediately upon moving to a new location on the sample. The HafSOx film thickness, measured to be 12−13 nm from spectroscopic ellipsometry measurements, agrees with the thickness and uniformity observed in these TEM images. Films are observed to change under prolonged exposure to the high-energy electron beam during analysis. A comparison of panels b and c of Figure 1, for example, reveals that the HafSOx/SiO_x bilayer thickness increases from approximately 15 to 17 nm after a 5 min exposure. In this process, the HafSOx film thickness decreases from 12 to 9 nm, while the SiO_x film thickness increases from 3 to 8 nm. This indicates that the electron beam is driving densification of the HafSOx layer while promoting further oxidation of the Si substrate. In the EDS line scan (Figure 1d), the S signal is found to track that of Hf, where S as a sulfate appears to be homogeneously distributed with Hf throughout the thickness of the film. This distribution is consistent with imaging results, and it confirms the high uniformity of the films in terms of both morphology and composition.

TEM images and STEM−EDS chemical analysis data of a HafSOx film, baked at 80 °C, exposed at 800 $\mu C/cm^2$, soaked in 25% TMAH(aq), and baked at 300 °C, are shown in Figure 2. A low-resolution image (Figure 2a) indicates that the resulting film remains uniform and very smooth, similar to that of the unexposed film. From the high-resolution image (Figure 2c), the exposed film is found to be amorphous, and its thickness relative to an unexposed film (Figure 1b) decreases from approximately 12 to 7 nm. From the STEM−EDS line scan, sulfate (S) is no longer present in the film, following the

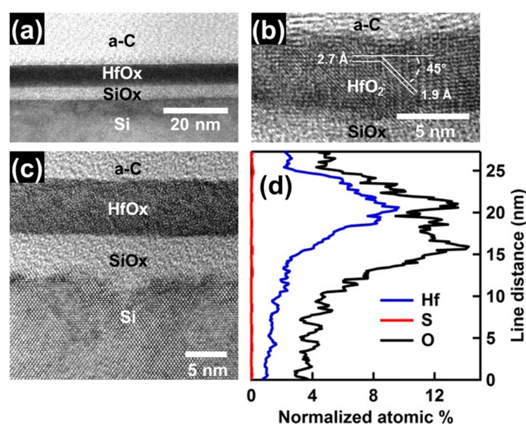

Figure 2. (a−c) TEM cross-sectional images of HafSOx film exposed at 800 $\mu C/cm^2$, soaked in 25% TMAH, and hard baked at 300 °C and (d) STEM−EDS line scan aligned to panel c.

soak in TMAH. These data indicate that electron-beam exposure and TMAH(aq) development have led to the formation of a thin, amorphous binary hafnium oxide hydroxide film. We also found that extended exposure of these films to the electron beam caused portions to crystallize (Figure 2b), producing atomic spacings consistent with monoclinic HfO_2.

XPS has been used to further elucidate composition and chemical state of the films. Hf 4f, S 2p, and O 1s spectra were monitored at four stages during the patterning process: (i) 80 °C post-application bake (PAB), (ii) 80 °C PAB and electron-exposure dose of 800 $\mu C/cm^2$, (iii) 300 °C PAB, and (iv) 80 °C PAB, exposure dose of 800 $\mu C/cm^2$, soak in TMAH, and 300 °C post-soak bake. Results are summarized in Figure 3.

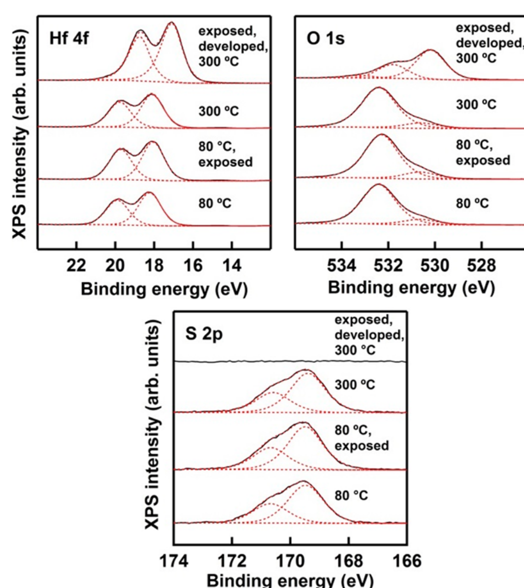

Figure 3. Hf 4f, O 1s, and S 2p X-ray photoelectron spectra of HafSOx films under selected process conditions.

Only subtle changes are observed in the relative intensities and binding energies of each element following only exposure and baking (80 °C, 80 °C and exposed, and 300 °C). After exposure and soaking in TMAH, however, significant spectral changes have occurred. For example, the O 1s and Hf 4f peaks shift to lower binding energies, and the S 2p peak is now absent, indicating significant chemical changes, including the loss of sulfate from the film. For the O 1s spectra, the low-binding-energy peak at 530.2 eV can be assigned to oxygen bound to Hf as oxide, while the high-binding-energy O 1s peak near 531.8 eV can be assigned to O bound as sulfate and hydroxo groups. Similar assignments have been made previously for Zr analogues of HafSOx.[17,18] For this sample, a third low-intensity peak at 533.3 eV was necessary to obtain an adequate fit; it is assigned to residual water that is present following the development process. This O 1s binding energy is consistent with water adsorbed to metal oxide surfaces.[19,20] We found that the low-binding energy metal oxide component becomes dominant after both exposure and TMAH soak. A similar change in the O 1s spectra was observed after the thermal desorption of sulfate from HafSOx films in ultrahigh vacuum.[21] While most of the oxygen is coordinated as Hf−O, a significant number of OH groups are detected following the 300 °C bake, which may be partly attributed to surface contamination from exposure to ambient prior to analysis. Together, the XPS and STEM−EDS analyses indicate that a fully exposed and developed HafSOx film is converted into a hafnium oxide hydroxide product.

We have extended these findings to examine fine-scale patterning of 9 nm wide lines using electron-beam lithography to write the lines at defined spacing by following the same processing steps as those used for the blanket films. A cross-sectional TEM image, representing decreasing line spacing from 44 to 11 nm, is shown in Figure 4a. The average full width

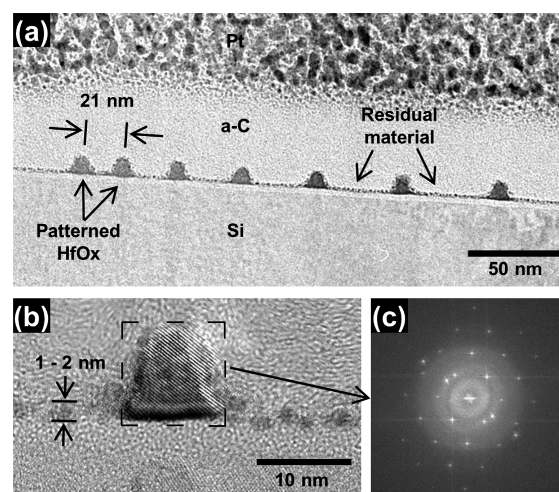

Figure 4. (a) TEM cross-sectional image of an electron-beam patterned HafSOx film after 800 $\mu C/cm^2$ exposure and development in 25% TMAH, (b) HR-TEM image of single line, and (c) fast Fourier transform of the region indicated in panel b.

at half maximum (FWHM) line width is 9.0 ± 0.7 nm. The features are readily resolved to the smallest spacing of 11 nm and a line−line distance of 21 nm. The rounded profiles reflect the modest development contrast of the system.[2] Initially, the as-processed features are amorphous, i.e., similar to the blanket film (Figure 2). After extended electron-beam exposure, the features are found to crystallize as monoclinic HfO_2 (Figure 4b). A Fourier transform (Figure 4c) of the atomic-resolved image indicates that the grain is oriented along the [101] zone axis. A very thin layer of residual material containing Hf is consistently observed between the lines, independent of spacing (Figure 4a). The TEM image of Figure 4b indicates that this residual is 1−2 nm thick and consists of small, discrete

structures. HafSOx precursor solutions contain nanosized clusters (diameter ≈ 1 nm), and remnants of individual nanoclusters may become strongly bound to the substrate during the patterning process. At all of the line spacings, secondary electrons can also initiate exposure chemistry.

This exposure could enhance interactions between the deposited film and the substrate or simply render these regions insoluble during development. A small increase in residual material thickness is observed at the smallest line spacing, where the thinnest portion is 2 nm. The image contrast is darker and more uniform relative to that of the discrete structures between the more widely space lines (Figure 4b). The buildup and broadening of the profile tails between the patterned lines are likely due to proximity effects associated with scattered electrons.

Overall, the findings can be well-correlated to the chemistry expected for the HafSOx system, i.e., $Hf(OH)_{1.6}(O_2)_{0.5}(SO_4)_{0.7}\cdot qH_2O$. The binding of peroxide and sulfate to Hf in small nanosized clusters inhibits olation and condensation reactions. As demonstrated, exposure to radiation drives peroxide decomposition,[22] inducing condensation reactions that lead to diminished solubility in TMAH(aq). However, this radiation-induced condensation does not lead to full densification, because sulfate remains a mobile species. Because the films are solid acids, they are neutralized on contact with TMAH(aq), resulting in extraction of sulfate. This sulfate is replaced with −OH, which sets the stage for additional condensation. The insolubility of the final product is thus initiated by both radiation and the follow-on development chemistry.

CONCLUSION

In this study, we have demonstrated the utility of high-resolution imaging and composition-mapping techniques for examining selected chemical steps contributing to the direct patterning of an inorganic material at feature sizes near 10 nm. The techniques have been successfully used to identify key aspects of condensation, sulfate exchange, and residual formation that contribute to pattern fidelity within the HafSOx system. We expect that the methods discussed herein will provide important information in future studies addressing near atomic-scale characterization of new classes of inorganic materials that hold promise for patterning at unprecedented resolutions.

AUTHOR INFORMATION

Corresponding Authors

*E-mail: greg.herman@oregonstate.edu.
*E-mail: douglas.keszler@oregonstate.edu.

Notes

The authors declare no competing financial interest.

ACKNOWLEDGMENTS

This material is based on work in the Center for Sustainable Materials Chemistry, which is supported by the U.S. National Science Foundation under Grant CHE-1102637. The authors thank Stephen Meyers, Jeremy Anderson, and Kai Jiang for several insightful discussions and Pete Eschbach for assistance with the electron microscopy work. Darren W. Johnson is a Scialog Fellow of Research Corporation for Science Advancement.

REFERENCES

(1) Anderson, J. T.; Munsee, C. L.; Hung, C. M.; Phung, T. M.; Herman, G. S.; Johnson, D. C.; Wager, J. F.; Keszler, D. A. Solution-processed HafSOx and ZircSOx inorganic thin-film dielectrics and nanolaminates. *Adv. Funct. Mater.* **2007**, *17*, 2117−2124.

(2) Stowers, J.; Keszler, D. A. High resolution, high sensitivity inorganic resists. *Microelectron. Eng.* **2009**, *86*, 730−733.

(3) Telecky, A.; Xie, P.; Stowers, J.; Grenville, A.; Smith, B.; Keszler, D. A. Photopatternable inorganic hardmask. *J. Vac. Sci. Technol., B: Nanotechnol. Microelectron.: Mater., Process., Meas., Phenom.* **2010**, *28*, C6S19−C6S22.

(4) Thrun, X.; Choi, K. H.; Freitag, M.; Grenville, A.; Gutsch, M.; Hohle, C.; Stowers, J. K.; Bartha, J. W. Evaluation of direct patternable inorganic spin-on hard mask materials using electron beam lithography. *Microelectron. Eng.* **2012**, *98*, 226−229.

(5) Ekinci, Y.; Vockenbuder, M.; Hojeij, M.; Wang, L.; Mojarad, N. M. Evaluation of EUV resist performance with interference lithography towards 11 nm half-pitch and beyond. *Proc. SPIE* **2013**, *8679*, 867910−867910.

(6) Grigorescu, A. E.; Hagen, C. W. Resists for sub-20-nm electron beam lithography with a focus on HSQ: State of the art. *Nanotechnology* **2009**, *20*, 292001.

(7) Haller, I.; Hatzakis, M.; Srinivasan, R. High-resolution positive resists for electron-beam exposure. *IBM J. Res. Dev.* **1968**, *12*, 251−256.

(8) Chen, W.; Ahmed, H. Fabrication of 5−7 nm wide etched lines in silicon using 100 keV electron beam lithography and polymethylmethacrylate resist. *Appl. Phys. Lett.* **1993**, *62*, 1499−1501.

(9) Vieu, C.; Carcenac, F.; Pepin, A.; Chen, Y.; Mejias, M.; Lebib, A.; Manin-Ferlazzo, L.; Couraud, L.; Launois, H. Electron beam lithography: Resolution limits and applications. *Appl. Surf. Sci.* **2000**, *164*, 111−117.

(10) Nishida, T.; Notomi, M.; Iga, R.; Tamamura, T. Quantum wire fabrication by e-beam elithography using high-resolution and high-sensitivity e-beam resist ZEP-520. *Jpn. J. Appl. Phys., Part 1* **1992**, *31*, 4508−4514.

(11) Tanenbaum, D. M.; Lo, C. W.; Isaacson, M.; Craighead, H. G.; Rooks, M. J.; Lee, K. Y.; Huang, W. S.; Chang, T. H. P. High resolution electron beam lithography using ZEP520 and KRS resists at low voltage. *J. Vac. Sci. Technol., B: Microelectron. Nanometer Struct.—Process., Meas., Phenom.* **1996**, *14*, 3829−3833.

(12) Ito, H. Chemical amplification resists for microlithography. *Adv. Polym. Sci.* **2005**, *172*, 37−245.

(13) Namatsu, H.; Takahashi, Y.; Yamazaki, K.; Yamaguchi, T.; Nagase, M.; Kurihara, K. Three-dimensional siloxane resist for the formation of nanopatterns with minimum linewidth fluctuations. *J. Vac. Sci. Technol., B: Microelectron. Nanometer Struct.—Process., Meas., Phenom.* **1998**, *16*, 69−76.

(14) Trikeriotis, M.; Bae, W. J.; Schwartz, E.; Krysak, M.; Lafferty, N.; Xie, P.; Smith, B.; Zimmerman, P. A.; Ober, C. K.; Giannelis, E. P. Development of an inorganic photoresist for DUV, EUV, and electron beam imaging. *Proc. SPIE* **2010**, *7639*, 76390E−76390E.

(15) Saifullah, M. S. M.; Khan, M. Z. R.; Hasko, D. G.; Leong, E. S. P.; Neo, X. L.; Goh, E. T. L.; Anderson, D.; Jones, G. A. C.; Welland, M. E. Spin-coatable HfO_2 resist for optical and electron beam lithographies. *J. Vac. Sci. Technol., B: Microelectron. Nanometer Struct.—Process., Meas., Phenom.* **2010**, *28*, 90−95.

(16) Broers, A. N.; Hoole, A. C. F.; Ryan, J. M. Electron beam lithography—Resolution limits. *Microelectron. Eng.* **1996**, *32*, 131−142.

(17) Hino, M.; Kurashige, M.; Matsuhashi, H.; Arata, K. The surface structure of sulfated zirconia: Studies of XPS and thermal analysis. *Thermochim. Acta* **2006**, *441*, 35−41.

(18) Breitkopf, C.; Papp, H.; Li, X.; Olindo, R.; Lercher, J. A.; Lloyd, R.; Wrabetz, S.; Jentoft, F. C.; Meinel, K.; Förster, S.; Schindler, K.-M.; Neddermeyer, H.; Widdra, W.; Hofmann, A.; Sauer, J. Activation and isomerization of *n*-butane on sulfated zirconia model systems—An integrated study across the materials and pressure gaps. *Phys. Chem. Chem. Phys.* **2007**, *9*, 3600−3618.

(19) Henderson, M. A. The interaction of water with solid surfaces: Fundamental aspects revisited. *Surf. Sci. Rep.* **2002**, *46*, 1−308.
(20) Herman, G. S.; Kim, Y. J.; Chambers, S. A.; Peden, C. H. F. Interaction of D_2O with CeO_2(001) investigated by temperature-programmed desorption and X-ray photoelectron spectroscopy. *Langmuir* **2009**, *15*, 3993−3997.
(21) Flynn, B.; Kim, D.; Clark, B. L.; Telecky, A.; Arnadottir, L.; Szanyi, J.; Keszler, D. A.; Herman, G. S. In-situ characterization of aqueous-based hafnium oxide hydroxide sulfate thin films. *Surf. Interface Anal.* **2013**, DOI: 10.1002/sia.5205.
(22) Okamoto, H.; Ishikawa, A.; Kudo, T. Photoresist characteristics and their reaction mechanism for crystalline peroxopolytungstic acid. *J. Electrochem. Soc.* **1989**, *136*, 2646−2650.